RESEARCH ARTICLE

Influence Of Laser Energy On Structural And Optical Properties Of $ZnO_{(x)}:NiO_{(1-x)}$ Films PreparedBy PulseLaser Deposition

Muna A. Issa[1,2] · Kadhim A. Aadim[1]

Abstract

The current study illustrates the $ZnO_{(x)}:NiO_{(1-x)}$ thin film synthesis using pulsed laser deposition at two different energy levels, 800 and 1000 mJ. The characteristics of the synthesized ZnO-NiO mixture were determined. XRF analysis obviously proved the presence of ZnO and NiO in thin film, with a high concentration ratio of Zn to Ni, suggesting minimal loss of these elements during the preparation process. The formation of the $ZnO_{(x)}: NiO_{(1-x)}$ thin film was achieved successfully and confirmed by characterization techniques. Peaks corresponding to hexagonal face-centered ZnO at 100, 002, 101, and 102° planes and cubic face-centered NiO at 111 and 200° were observed in XRD patterns. A comparison between the energy levels and their impact on the properties of the mixture, as determined by XRD and AFM analysis, indicated a reduction in particle size with increased energy, as well as a decrease in the values of root mean square (RMS) and average roughness. Additionally, optical properties showed an increase in absorbance with higher energy levels and the value of energy gap 3.85 for energy level 1000 mJ and 4.1 for 800 mJ.

Introduction

The chemical compound zinc oxide (ZnO) is made up of zinc and oxygen atoms. Zinc oxide (ZnO) nanoparticles are tiny particles with dimensions typically ranging from 1 to 100 nm and have unique properties in comparison to bulk ZnO, attracting interest in a variety of sectors [1, 2]. Their properties are attributed to their large surface area relative to their volume, acquiring the capicity to be used in biomedicine, optoelectronics, energy storage, flexible electronics, photocatalysis, and sensors [3]. ZnO-NPs have been discovered to possess powerful antimicrobial properties, which makes them promising for usage in medical applications, such as antimicrobial coatings and wound dressings. Additionally, ZnO nanoparticles demonstrate remarkable optical characteristics, which includes visible light emission (photoluminescence) and strong UV absorption. They are employed in solar cells, LED lighting, water purification systems, and medical devices [4, 5]. Although ZnO nanoparticles have many difficulties in their synthesis and scalability, they can enhance innovation and provide solutions to a wide range of environmental and technical issues.

Using pulsed laser deposition (PLD) in synthesizing ZnO thin films provides outstanding properties that make them suitable for a wide range of applications, such as high crystallinity, customized shape, homogeneity, accurate thickness control, stoichiometric composition, powerful adhesion, and adaptability on various substrates [6]. On the other hand, nickel oxide (NiO) nanoparticles have unique properties useful in various fields [7]. There are many ways to synthesize these nanoparticles, such as sol-gel and chemical precipitation procedures. They are found to be used as a catalyst in chemical reactions as well as semiconductors in electronics and optoelectronics. They have significant applications in the biological and energy storage sectors, and their gas sensitivity enables them for gas sensing applications [8].

PLD produces nickel oxide (NiO) thin films with special qualities, offering an accurate control of growth rate while also confirming strong substrate surface adherence. NiO

✉ Muna A. Issa
muna.ahmed@sc.uobaghdad.edu.iq

[1] Department of Physics, College of Science, University of Baghdad, Baghdad, Iraq

[2] Quality Assurance and Performance Evaluation Department, Mustansiriyah University, Baghdad, Iraq

thin films synthesized by PLD showed also high crystallinity, stoichiometric composition, homogeneity, and strong adherence to substrate surfaces by precisely controlling the thickness, shape, and composition of the film [9–12]. Since they generally show outstanding optical transparency, NiO thin films are perfect for optoelectronic applications. Furthermore, they can be used in medical field by modifying their design which enhance their ability to combat microorganisms, efficiently deliver medications, and interact effectively with biological tissues. By incorporating nickel oxide into zinc oxide matrix, the reactivity of the composite and surface characteristics can be enhanced, making it suitable for various medical applications. These could include coatings to prevent infections on medical devices, implants, or wound dressings, as well as techniques for delivering drugs in a controlled and targeted way [13]. Furthermore, they have interesting optical properties for diagnostic applications and biological imaging. In this work, two different laser energies will be used to study the structure and properties associated to light of a composite having a zinc oxide to nickel oxide ratio of 0.3. Our goal is to evaluate how different laser energies affect these properties.

Details of the project

A mixture of Zinc oxide and nickel oxide was prepared with a concentration of x = 0.3. Figure 1 shows the ratio of these elements by using the ratio equation. The powders were combined with a gate mortar for an hour to make sure

$W_{Zn} = 65.409 \, g/mol$, $W_{Ni} = 58.693 \, g/mol$, $W_O = 16 \, g/mol$

$ZnO_x : NiO_{(1-x)}$, At x = 0.3

$W_{ZnO:NiO} = (65.409 + 16)*0.3 + (58.693 + 16)*0.7$

$\quad = 81.409*0.3 + 74.693*0.7$

$\quad = 24.422 + 52.285$

$\quad = 76.707/2$

$\quad = 38.353$

$\quad = 24.422/38.353 + 52.285/38.353$

$\quad = 0.63 + 1.36$

$\quad = 0.6_{ZnO} , 1.4_{NiO}$

Fig. 1 The method followed to determine the ratio of 0.3 for ZnO: NiO thin film

homogeneity and cohesion. Then, to create 20 mm-diameter pellets, the mixture was compressed using a hydraulic press for 10 min at 6 Pa. PLD was used to apply thin ZnO coatings on glass substrates that were $75 \times 25 \times 1.2$ mm. Pulsed laser ablation deposition is one of the best and most affordable methods for depositing metals, semiconductors, and their derivatives [14]. Using 500 shots by a focusing-YAG laser, a pure ZnO: NiO target was pulsed under parameters as following in a vacuum chamber during the PLD process: repetition rate of 6 Hz, wavelength of 1064 nm, laser energy between 800 and 1000 mJ, and maximal period of 9 ns. In order to maximize the area of deposition on the glass base, the laser pulses should be directed at the target material's surface at an angle of incidence of 45 degrees. The methodology involved the deposition of thin coatings at any discharge height while subjected to a pressure of 10^{-2} Torr in a glass cylindrical chamber measuring 30 cm in diameter and 40 cm in height [15, 16]. In order to ascertain the thickness of the strata to be 200 nm, the optical interferometer method was used. In order to manipulate the structure and morphology of the deposited materials at the nano-metric scale, several critical parameters must be adjusted. These consist of laser flounce, constitution of the background atmosphere, pressure, target-to-substrate distance, substrate temperature, and pulses number [17]. In Fig. 2, the workflow is shown.

W $_{ZnO}$	W $_{NiO}$	Total weight
0.6 gm	1.4gm	2gm

Fig. 2 Steps of work for PLD method
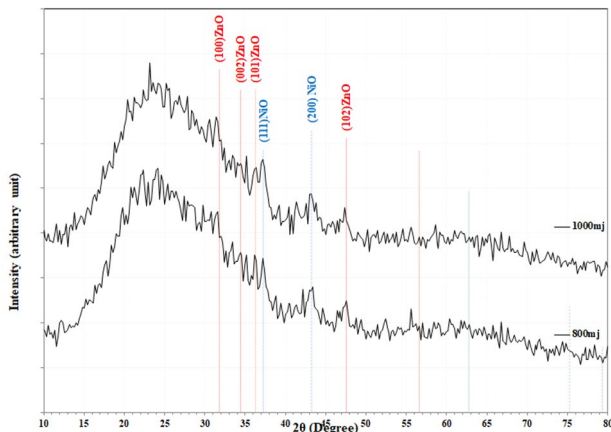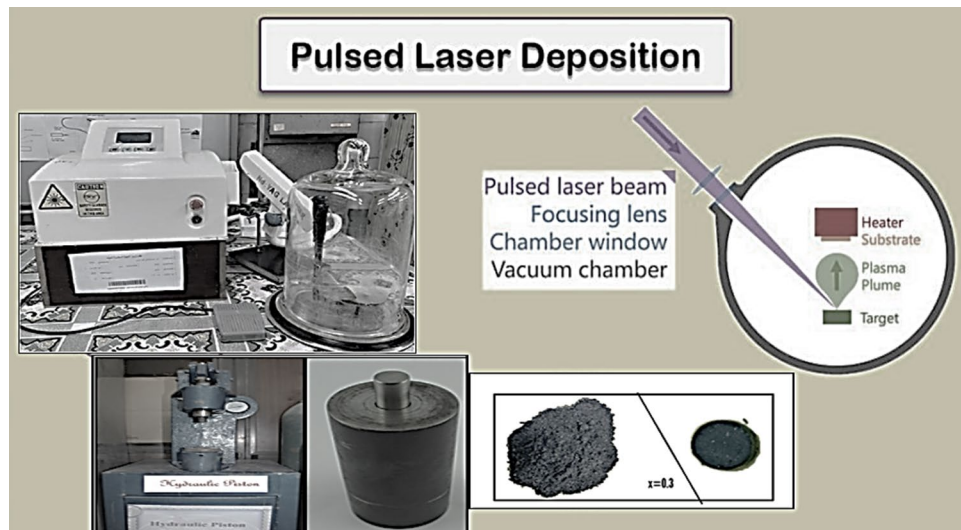
Fig. 3 XRD patterns of $ZnO_{(x)}:NiO_{(1-x)}$ at x = 0.3 thin film

Results and discussion

X-ray is used to determine the crystal structure of materials. When X-rays pass through a crystalline material, they are scattered specifically according to the atomic arrangement, which helps in determining the crystal structure and compounds Fig. 3 presents the patterns of XRD diffraction of synthesized ZnO(x) (1-x) nanoparticle films with x = 0.3, deposited on a glass substrate. Peaks corresponding to cubic face-centered NiO at 111 and 200° and hexagonal face-centered ZnO at 100, 002, 101, and 102° planes were seen in the XRD patterns for the ZnO(x) (1-x) film. These patterns were compared to ZnO (JCPDS file No. 96-901-1663) and NiO (JCPDS file No. 96-432-0488) standard X-ray diffraction data files [18, 19]. The values of, mean crystallites size, full width at half maximum FWHM, and Miller indices (hkl) are listed in Table (1). FWHM represents the width of a peak in the spectroscopic analysis, such as material deposition distribution or laser beam intensity profile. FWHM increases with higher laser energy due to increased target material heating, broadening thermal plumes and material distribution [20]. Conversely, higher energy enhances ablation efficiency, ejecting smaller particles from the target surface, resulting in smaller grain sizes [21]. The results shown in Table 2 confirm that increasing energy leads to smaller particles.

Table 1 Summery of X-ray characterization for $ZnO_{(x)}:NiO_{(1-x)}$ at x = 0.3

sample	2θ (Deg.)	FWHM (Deg.)	d_{hkl} Exp.(Å)	C.S (nm)	hkl	Phase
800 mJ	31.5645	0.6200	2.8322	13.3	(100)	Hex. ZnO
	34.4165	0.6300	2.6037	13.2	(002)	Hex. ZnO
	36.2595	0.4420	2.4755	18.9	(101)	Hex. ZnO
	37.2355	0.6200	2.4128	13.5	(111)	Cub. NiO
	43.2475	0.6300	2.0903	13.6	(200)	Cub. NiO
	47.5275	0.6320	1.9116	13.7	(102)	Hex. ZnO
1000 mJ	31.5765	0.6529	2.8311	12.7	(100)	Hex. ZnO
	34.4285	0.6634	2.6028	12.5	(002)	Hex. ZnO
	36.2715	0.4654	2.4747	18.0	(101)	Hex. ZnO
	37.2475	0.6529	2.4121	12.8	(111)	Cub. NiO
	43.2595	0.6634	2.0898	12.9	(200)	Cub. NiO
	47.5395	0.6655	1.9111	13.0	(102)	Hex. ZnO

Table 2 Summery of AFM characterization

Sample		RATIO	ENERGY (mj)	Grain size (nm)	RMS roughness (nm)	Roughness Ave. (nm)
ZnO$_{(x)}$:NiO$_{(1-x)}$	x = 0.3		800	78.595	8.44899	5.56299
			1000	15.4014	2.11014	1.43785

The findings of the X-ray fluorescence (XRF) investigation are displayed in Fig. 4. The concentrations of Ni and Zn were 98.03% and 98.50%, respectively, according to their spectral lines. The absence of the oxygen (O) spectra in the figure may be caused because of the low atomic number of oxygen (8). About 1% of residual oxygen remained, along with traces of other elements that were considered impurities [22]. The high concentration ratio of zinc to nickel reveals that there was little loss in the sample structure and that most of the zinc and nickel added during the preparation procedure was preserved. ZnO and NiO were verified by this analysis.

Figure 5; Table 2 provide evidence that as the energy increases in ZnO: NiO composite, the grain size tends to decrease, resulting in the formation of smaller crystalline grains. The RMS roughness, which quantifies surface irregularities, can also decrease in certain cases with increased energy [23]. Likewise, Roughness Average (RA), another measure of surface roughness, may decrease as well, attributed to the smoothing of surface features or refinement of grain structure caused by the heightened energy. This ultimately leads to a smoother overall surface. and The best is when the laser energy is 1000 mj, as this energy leads to greater effects and noticeable changes in the material, making it more effective.

Scanning electron microscopy is crucial for studying the morphology of nanoparticles, as their shape, surface area, and size directly impact their antibacterial properties. Smaller nanoparticles are particularly effective due to their improved penetration and interaction of microorganisms. Furthermore, the physical harm or destruction of cell membranes can be caused by the morphology of nanoparticles, such as their sharp edges or protrusions. In the case of the ZnO$_{(x)}$:NiO$_{(1-x)}$ composite material at x = 0.3, depicted in Fig. 6, spherical nanostructures with significant particle agglomeration are observed. The Nano composite particles, on average, ranged from 10.19 to 23.2 nm in diameter for 800 mJ and from 12.89 to 32.86 nm for 1000 mJ.
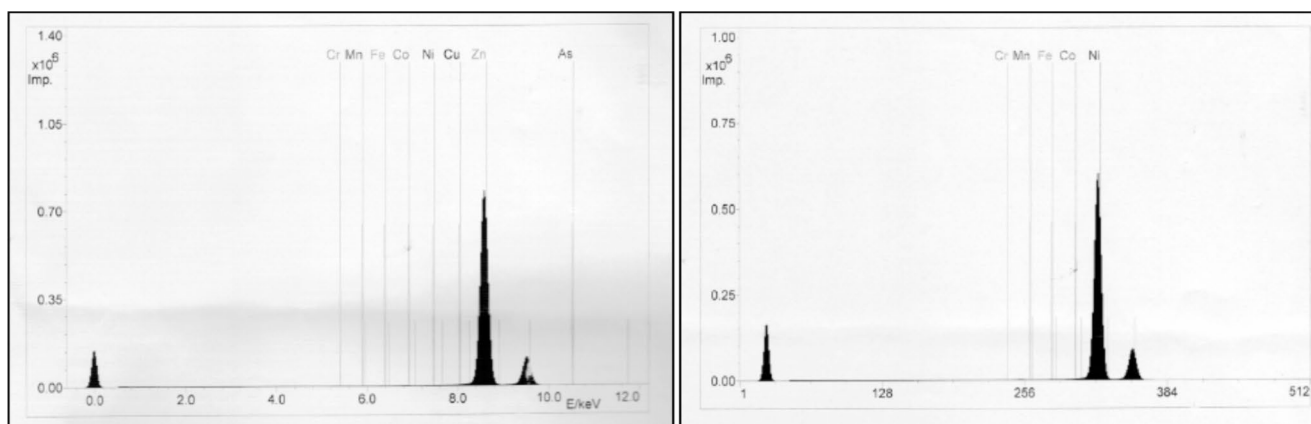
Fig. 4 XRF of ZnO and NiO
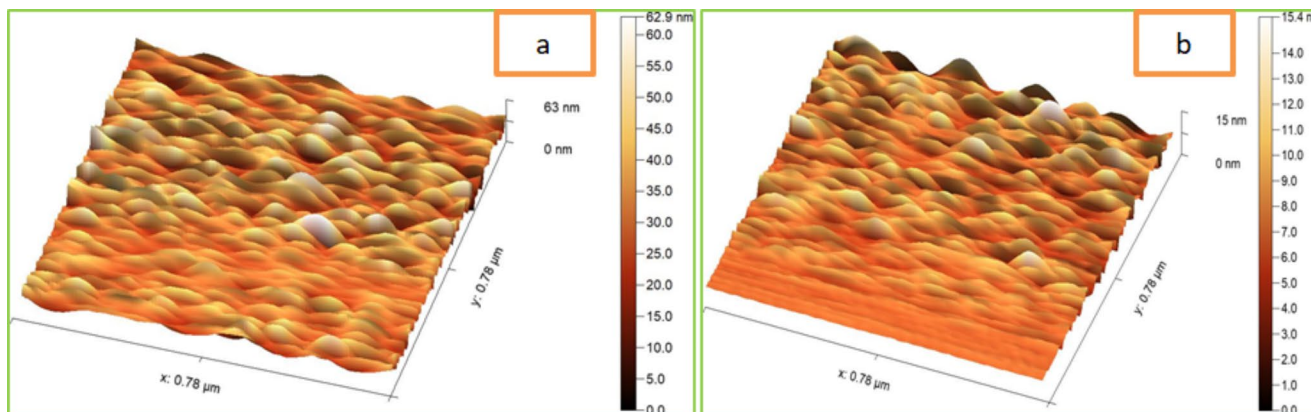
Fig. 5 AFM of ZnO$_{(x)}$:NiO$_{(1-x)}$ at x = 0.3, (a) in 800 mJ and (b) in 1000 mJ
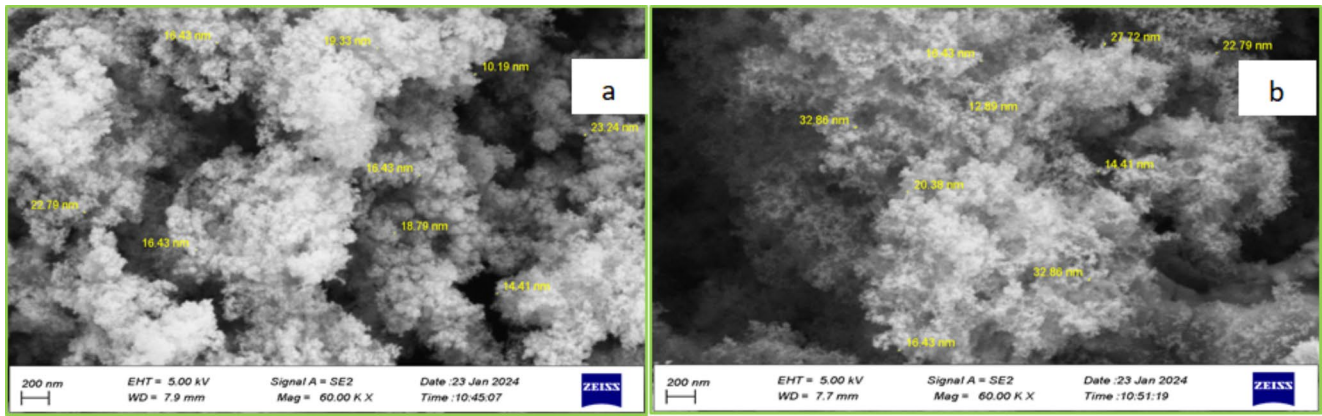
Fig. 6 SEM image of ZnO$_{(x)}$:NiO$_{(1-x)}$ at x = 0.3, for a) 800 mJ and b)1000 mj
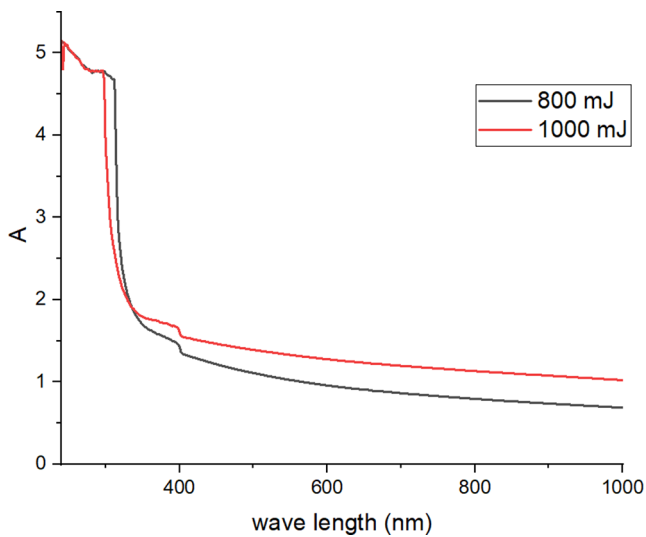

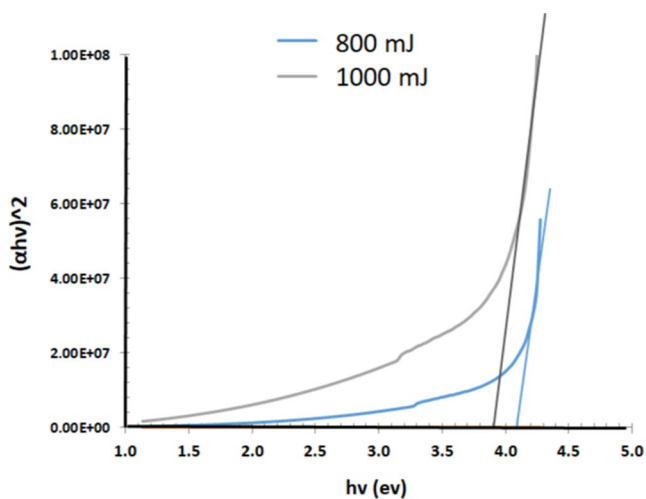**Fig. 7** UV-visible absorption spectra of ZnO$_{(x)}$:NiO$_{(1-x)}$ at x = 0.3

Fig. 8 The measurement of energy gap

Figure 7 illustrates the ultraviolet-visible absorption spectra of the ZnO$_x$:NiO$_{1-x}$ composite at x = 0.3 for energy levels of 800 mJ and 1000 mJ. The findings indicate that higher energy facilitates a more effective transfer of material from the target to the substrate, resulting in heightened absorbance. Both ZnO and NiO exhibit optical absorption below 400 nm, indicating their capacity to absorb ultraviolet (UV) radiation. The band gap can be determined using the equation that follows, as shown in Fig. 8 (1).

$$(\alpha h\nu) = A (h\nu - Eg) n \qquad (1)$$

where α, h, A, ν, Eg, and n represent the material absorption coefficient, Planck's constant, frequency, the band gap energy, the proportionality constant, and the type of sample transitions (direct or indirect), respectively [24, 25].

The optical energy band gap of ZnO: NiO nano-composite was found to vary depending on the energy input during fabrication. At 800 mJ, the band gap measured 4.1 eV, while at 1000 mJ, it decreased to 3.85 eV, which agrees with the results of [26]. This decrease in band gap at higher energy inputs suggests that the energy of the ablated species is significant, potentially leading to increased atomic mobility and rearrangement of atoms during the film deposition process [27]. These changes in atomic arrangement may have an impact on the deposited material's energy band structure, which could lead to a narrowing of the energy gap.

Conclusions

Utilizing the PLD approach presents a sustainable, cost-efficient, and readily scalable method for manufacturing ZnO: NiO thin film. The great purity of the metal oxides created using this approach is confirmed by the XRF analysis. XRD patterns were observed showing peaks for NiO cubic face-centered and for ZnO hexagonal face-centered structure.

The mean crystallite size and peak width at half-maximum FWHM were determined. With increasing energy, the crystal grain size decreased, and the SEM images showed spherical nanostructures. It was discovered that the optical emitting energy gap of the composite material changes with the energy used in the preparation.

Author contributions MAI contributed to the formation of thin zinc oxide: Nickel oxide films and carried out the required tests to study zinc oxide's optical and structural properties. As for KAA, he completely supervised (the work method, wrote the research, and analyzed the results).

Data availability This study did not generate or examine any datasets, so data sharing is not relevant to it.

Declarations

Ethical approval The authors certify that there is not any conflict of interests.

Competing interests There are no known conflicts of interest on the part of the writers.

References

1. K.A. Aadim, A.Z. Mohammad, M.A. Abduljabbar, Influence of laser energy on synthesizes of CdO/Nps in liquid environment, IOP conf. Ser. Mater. Sci. Eng. **454**, 012028 (2018)
2. D.T. Mohammed, G.H. Mohammed, Investiagtion of structural, optical and electrical properties of MnO doped with Cu thin films prepared by PLD technique for solar cell applications, East European Journal of Physics, 2023(3), 391–399(2023)
3. M.P. Hernandez, G. Hernández, ,quantitative surface morphology analysis using roughness parameters. Revista Cubana De Física. **38**(1), 10–16 (2021)
4. J. Theerthagiri, S. Salla, R.A. Senthil, P. Nithyadharseni, A. Madankumar, P. Arunachalam, H.S. Kim, A review on ZnO nanostructured materials: energy, environmental and biological applications. Nanotechnology. **30**(39), 392001 (2019)
5. N.K. Abdaalameer, S.N. Mazhir, K.A. Aadim, Diagnostics of zinc selenite plasma produced by FHG of a q-switchednd: Yaglaser. Chalcogenide Lett. **18**(7), 405–411 (2021)
6. M.A. Essa, K.A. Aadim, Structural and optical properties of SnO2 doped ZnO thin films prepared by pulsed nd: YAG Laser Deposition. Iraqi J. Phys. **17**(42), 125–135 (2019)
7. M. Mohammed, Synthesis and characterization of Nickel Oxide nanoparticles by Green as well as chemical routes and comparisons their Properties. Iraqi J. Nat. Sci. Nanatechnol. **4**, 54–63 (2023)
8. K.J. Shailja, Singh, R.C. Singh, Highly sensitive and selective ethanol gas sensor based on Ga-doped NiO nanoparticles. J. Mater. Sci.: Mater. Electron. **32**, 11274–11290 (2021)
9. H.J. Imran, K.A. Hubeatir, K. Aadim, A., a novel method for ZnO@ NiO core–shell nanoparticle synthesis using pulse laser ablation in liquid and plasma jet techniques. Sci. Rep. **13**(1), 5441 (2023)
10. M.A. Khalaf, B.M. Ahmed, K.A. Aadim, Spectroscopic analysis of $CdO_{1-X}:Sn_X$ plasma produced by nd: YAG laser. Iraqi J. Sci. **61**(7), 1665–1671 (2020)
11. R.S. Mohammed, K.A. Aadim, Ahmed,Estimation of in vivo toxicity of MgO/ZnO core/shell nanoparticles synthesized by eco-friendly non-thermal plasma technology. Appl. Nanosci. **12**(12), 3783–3795 (2022)
12. M.H. Dwech, K.A. Aadim, L.A. Hamid, Influence of laser energy on the characteristics of Ag2S/ITO thin films solar cell prepared by PLD technique, AIP Conference Proceedings, 2213, 020147(2020)
13. A. Sathiyaseelan, K.V. Naveen, X. Zhang, K. Han, M. Wang, H.,Research progress on chitosan-zinc oxide nanocomposites fabrication, characterization, biomedical and environmental applications. Coord. Chem. Rev. **496**, 215398 (2023)
14. K.A. Aadim, A.A. Yousef, Spectroscopic study of AL nitrogen plasma produced by DC glow discharge. Iraqi J. Sci. **59**(1 C), 494–501 (2018)
15. T.S. Hussein, A.F. Ahmed, K.A. Aadim, Spectroscopic analysis of CdO:Fe plasma generated by nd: YAG Laser. Iraqi J. Sci. **63**(2), 548–555 (2022)
16. K.A. Aadim, Detection of laser-produced tin plasma emission lines in atmospheric environment by optical emission spectroscopy technique. Photon Sens. **7**(4), 289–293 (2017)
17. K.A. Aadim, M.M. Shehab, Influence of Laser Energy on the Structural and Optical properties of (CdO):(CoO) Thin films Produced by Laser-Induced plasma (LIP). Iraqi J. Phys. **19**(49), 42–52 (2021)
18. A.S. Yasir, A.S. Hameed, N.J. Ridha, F.K.M. Alosfur, K.J. Tahir, R.A. Madlol, Enhancement of voltammetric properties of silver nanoparticles doped ZnO nanorods for glucose biosensing. J. Mater. Sci. Mater. Electron. **34**(4), 315 (2023)
19. A.S. Maktoof, G.H. Mohammed, The effect of au nanoparticles on the Structural and Optical properties of (NiO: WO3) thin films prepared by PLD technique. Iraqi J. Sci. **63**(6), 2502–2513 (2022)
20. M.A. Issa, K. Aadim, A.,Optical and structural characterization of ZnO: NiO nano composite prepared by pulsed laser deposition method. J. Opt., **1–6**(2024)
21. S.H. Jeong, O.V. Borisov, J.H. Yoo, X.L. Mao, R.E. Russo, Effects of particle size distribution on inductively coupled plasma mass spectrometry signal intensity during laser ablation of glass samples. Anal. Chem. **71**(22), 5123–5130 (1999)
22. K. Samudrala, S.B. Devarasetty, Effect of the copper on thermomechanical and optical properties of S-Se-Cu chalcogenide glasses, In IOP Conference Series: Materials Science and Engineering, 330(1), 012042(2018)
23. A.A. Almaula, Ç.Y. Ataol, G.H. Mohammed, Structural and optical properties Study of SnS: Ag Doped Cu Thin films prepared by PLD technique for solar cell application. J. Pharm. Negat. Results. **13**(4), 936–944 (2022)
24. M.M. Hameed, A.-M.E. Al-Samarai, K.A. Aadim, Synthesis and characterization of gallium oxide nanoparticles using pulsed laser deposition. Iraqi J. Sci. **61**(10), 2582–2589 (2020)
25. S. Haq, A.W. Raja, S.U. Rehman, A. Mezni, M. Ben Ali, A. Hedfi, P. Ahmad, Phytogenic synthesis and characterization of NiO-ZnO nanocomposite for the photodegradation of brilliant green and 4-nitrophenol, Journal of Chemistry, 2021, 1–10(2021)

26. J.M. Nel, F.D. Auret, L. Wu, M.J. Legodi, W.E. Meyer, M. Hayes, Fabrication and characterisation of NiO/ZnO structures. Sens. Actuators B **100**(1–2), 270–276 (2004)

27. S.M. Rossnagel ,Thin film deposition with physical vapor deposition and related technologies, Journal of Vacuum ScienceTechnology, A. Vacuum, Surfaces, and Films, 21(5), S74-S87(2003)